Temperature distribution in an oscillatory flow with a sinusoidal wall temperature

Eduardo Ramos [a,*], Brian D. Storey [b], Fernando Sierra [c], Raúl A. Zúñiga [c], Andriy Avramenko [c]

[a] *Center for Nonlinear Dynamics, The University of Texas at Austin, Austin, TX 78712, USA*
[b] *Franklin W. Olin College of Engineering, 1735 Great Plain Avenue, Needham, MA 02492-1245, USA*
[c] *Centro de Investigación en Energía—UNAM, Ap. P. 34, Temixco Morelos 62580, Mexico*

Received 18 October 2002

Abstract

The temperature field generated by an oscillatory boundary layer flow in the presence of a wall with a sinusoidal temperature distribution is analyzed. A linear perturbation method is used to find closed form analytical solutions for the temperature field when the amplitude of the velocity oscillation is small. The analytical solutions only consider long-time behavior when the temperature fields oscillate with the frequency of the flow. The structure of the equation that governs the temperature correction due to convection is similar to that of diffusive waves with the solution consisting of traveling or standing waves. The temperature distribution is also solved numerically which allows a description of the transient and periodic temperature fields. At short times, the solution has similarities with the traveling waves, while at long times the solution evolves toward a standing wave. As the amplitude of the solution is increased, beyond the linear approximation, the temperature oscillation remains periodic, but more Fourier modes are incorporated. We find that in all cases, the long-time, time averaged heat transfer from the boundary to the fluid is zero.
© 2004 Published by Elsevier Ltd.

1. Introduction

Since the mid-20th century numerous studies on axial and transverse diffusion in oscillatory flows have been conducted with a special emphasis on biological and geophysical applications. Recently, the potential to use oscillatory flows to augment the heat transfer rates in Stirling machines, cryocoolers and in computer components has renewed interest in the field. Progress in understanding heat transfer in oscillatory flows with zero mean (reciprocating flows) is incomplete since studies carried out by different groups have been motivated by specific applications and no general description and interpretation of the phenomenon is available.

Cooper et al. [1] and Zhao and Cheng [2] have published review papers that include much of the progress to date on reciprocating flows.

A general classification of the flows can be made by considering the geometry of heating (or cooling) at the boundaries. The first classification group includes heat transfer studies in ducts with walls of spatially uniform temperature. These studies are inspired by the classical example of heat transfer in a duct with hot walls and constant flow velocity which was solved originally by Nusselt and See [3]. A numerical solution of the heat transfer equations for a reciprocating laminar flow in a pipe with entrance effects was conducted by [4]. An interesting property of this flow with Prandtl number order one, is that annular effects similar to those found in the axial velocity distributions, were found for the temperature fields. The same authors performed experimental observations of this flow and reported space-cycle averaged Nusselt numbers that coincide with the

---
[*] Corresponding author. Permanent address: Centro de Investigación en Energía—UNAM, Ap. P. 34, Temixco Morelos 62580, Mexico.

numerical calculations [5]. A major experimental difficulty in this configuration is that inlet and outlet regions alternatively change roles and efficient heat removal mechanisms are required if the swept length is large.

The second group of studies is characterized by the assumption of a linear wall temperature profile. A reciprocating flow in such a duct can substantially increase the heat transferred between the ends of the duct. Due to the potential use of this configuration in a large number of applications, this problem has been studied in detail [6,7]. Heat transport in a boundary layer from an oscillating flat plate with a linear temperature gradient can achieve a large heat flux due to the interaction of a transverse conduction flux with the periodic longitudinal convection [8].

The third flow group we identify consists of heat transfer problems with nonlinear wall temperature distributions. The mechanisms of heat transfer in oscillatory flows in short rectangular ducts with a pulse function wall temperature distribution have been explored with experimental and numerical tools [9]. The oscillatory Nusselt number was found to be proportional to the length of the heated region and the third power of the oscillatory Reynolds number. Strong velocity and temperature fluctuations are attributed to sudden pressure changes at the channel outlets. In this flow it was observed that temperature and velocity fluctuations are out of phase. Heat transfer in oscillatory pipe flow with a sinusoidal wall temperature has been analyzed assuming that the wavelength of the temperature profile along the wall is larger than the radius of the pipe [10]. In this analysis, the axial velocity profile was averaged over the radius to provide a uniform axial velocity. With this crucial assumption, the total derivative for the temperature in the energy conservation equation can be transformed into a partial derivative with respect to time. The transformed energy equation was solved using Fourier series. The qualitative behavior was described in terms of two parameters: the ratio of the radius to the thickness of Stokes thermal boundary layer (thermal Womersley number) and the ratio of the swept length to the wavelength of the wall temperature. The validity of the assumptions on which the model is based has not been confirmed. In particular, the cross-section uniformity of the velocity is questionable since it is well known that the axial velocity varies in the radial direction and varies with the frequency.

In the present paper, we present an analysis of heat transfer in an oscillatory flow boundary layer where a sinusoidal temperature profile is prescribed at the wall. This problem is an example of the third group and is similar to that studied by Lee et al. [10], but we do not average the velocity along the transversal direction. Initially, we assume that the amplitude of the velocity of oscillation is small and solve for the temperature distribution using a perturbation method. In the linear case, we find that the temperature correction due to the oscillatory convection obeys a diffusion wave equation [11] whose solutions are traveling and standing waves. The case when the amplitude of oscillation is not small is analyzed with a numerical method. The analytical solution to the sinusoidal problem can be useful since under circumstances where the problem is linear, the superposition principle can be used to analyze arbitrary wall temperature profiles.

2. Analysis

Assume that a two-dimensional oscillatory flow exists in the semi-infinite plane above a rigid wall. The axial coordinate x is defined parallel to the wall and the transverse coordinate y runs perpendicular to it. A sinusoidal temperature profile of the form $T(x) = \overline{T} + \frac{T_w}{2}\cos(x/\lambda)$ is prescribed at the wall which is assumed to extend in the interval $-\infty < x < \infty$. $\overline{T}$ is a reference temperature equal to the average temperature of the wall, T_w is the amplitude of the temperature distribution at the wall and λ is the wavelength. We will assume that $|T_w| < \overline{T}$. This situation is schematically presented in Fig. 1.

Assuming that no natural convection effects are present, the velocity of the pulsating flow at a solid boundary has only an axial component and is given by [12]

$$u(y,t) = U_\infty \left[\cos(\omega t) - \exp\left[-\left(\frac{\omega}{2\nu}\right)^{1/2} y \right] \right.$$
$$\left. \times \cos\left(\omega t - \left(\frac{\omega}{2\nu}\right)^{1/2} y \right) \right] \qquad (1)$$
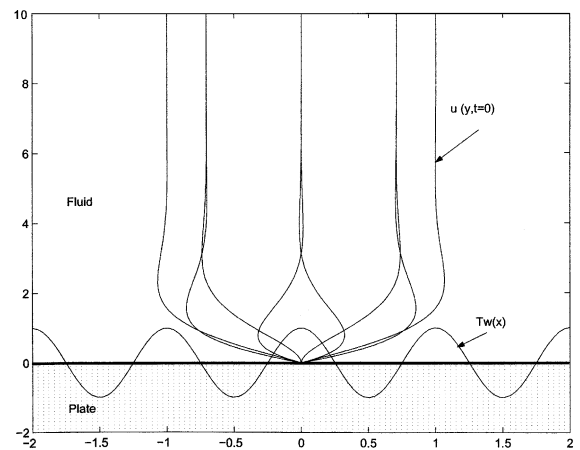

Fig. 1. Semi-infinite fluid region limited by a rigid plate with a sinusoidal temperature profile.

where U_∞ is the amplitude of the free stream velocity far away from the plate, ω is the oscillation frequency and v is the kinematic viscosity of the fluid.

Neglecting viscous heating and considering an incompressible fluid, the heat transfer equation for a two-dimensional flow is

$$\frac{\partial T}{\partial t} + u\frac{\partial T}{\partial x} + v\frac{\partial T}{\partial y} = \kappa\left(\frac{\partial^2 T}{\partial x^2} + \frac{\partial^2 T}{\partial y^2}\right)$$

where $\kappa = k/\rho C_p$ is the thermal diffusivity of the fluid.

Since the motion takes place only in the axial direction, the equation that describes the temperature field is

$$\frac{\partial T}{\partial t} + u(y,t)\frac{\partial T}{\partial x} = \kappa\left(\frac{\partial^2 T}{\partial x^2} + \frac{\partial^2 T}{\partial y^2}\right) \tag{2}$$

where $u(y,t)$ given by Eq. (1).

The boundary conditions are

$$T(x,0,t) = \overline{T} + \frac{T_w}{2}\cos\left(\frac{x}{\lambda}\right)$$

$$T(x,y\to\infty,t) = \overline{T}$$

We have assumed that the temperature of the free stream is equal to the average wall temperature. The boundary conditions in the x direction can be considered cyclic with a periodicity and phase dictated by the boundary conditions at the wall. We will now cast the equation into non-dimensional form using the symbol * to denote dimensionless quantities. The non-dimensional axial variable is defined by the wavelength of the wall temperature, $x^* = x/\lambda$. The natural scale for the transverse direction in an oscillatory boundary layer is the Stokes penetration depth, defined by $\delta = \sqrt{2v/\omega}$. The problem contains two time scales; the forcing time scale $1/\omega$, and the diffusive time scale, λ^2/v. Since the main objective of the present study is the effect of the forced convection, we will scale time with the frequency of oscillation i.e. $t^* = t\omega$. With this scaling, the limit $\omega \to 0$ is excluded from the analysis. Of course, this does not imply a singularity; the $\omega \to 0$ limit can be easily analyzed by the using diffusive time scale. The scaled velocity and temperature are $u^* = u/U_\infty$ and $T^* = (T - \overline{T})/T_w$ respectively.

Dropping the asterisks, the non-dimensional equation that governs the temperature distribution is

$$\frac{\partial T}{\partial t} + \epsilon u\frac{\partial T}{\partial x} = \frac{1}{PrR_\omega}\frac{\partial^2 T}{\partial x^2} + \frac{1}{2Pr}\frac{\partial^2 T}{\partial y^2} \tag{3}$$

where u is the non-dimensional version of Eq. (1). The relevant non-dimensional parameters are the Prandtl and oscillatory Reynolds numbers defined by

$$Pr = \frac{v}{\kappa} \tag{4}$$

$$R_\omega = \frac{\omega\lambda^2}{v} \tag{5}$$

and the parameter ϵ that reflects the importance of the convective effects:

$$\epsilon = \frac{Re}{R_\omega} = \frac{U_\infty}{\omega\lambda} \tag{6}$$

The Reynolds number (Re) is defined by $Re = U_\infty\lambda/v$ and does not appear as an independent parameter in the formulation. Note that an alternative interpretation of ϵ is $\epsilon = 1/St$, where the Strouhal number (St) is the ratio of inertial to forcing characteristic times. The non-dimensional boundary conditions are

$$T(x,0,t) = \tfrac{1}{2}\exp(ix)$$

$$T(x,y\to\infty,t) = 0$$

$$T(0,y,t) = T(2n\pi,y,t)$$

where $n = 1,2,3\ldots$

3. Solution for $\epsilon \ll 1$

The complete solution to Eq. (3) is difficult to obtain in analytic form, but an approximate solution can be calculated when the oscillatory flow is small.

We shall assume that the temperature field has the following form:

$$T = T_0(x,y) + \epsilon T_1(x,y,t) \tag{7}$$

and analyze only the case where $\epsilon \ll 1$.

Substituting Eq (7) in Eq (3), we get

$$\epsilon\frac{\partial T_1}{\partial t} + \epsilon u\frac{\partial T_0}{\partial x} + \epsilon^2 u\frac{\partial T_1}{\partial x} = \frac{1}{PrR_\omega}\frac{\partial^2 T_0}{\partial x^2} + \frac{1}{2Pr}\frac{\partial^2 T_0}{\partial y^2}$$
$$+ \frac{\epsilon}{PrR_\omega}\frac{\partial^2 T_1}{\partial x^2} + \frac{\epsilon}{2Pr}\frac{\partial^2 T_1}{\partial y^2} \tag{8}$$

The zero-order temperature distribution contains the terms where the parameter ϵ is absent

$$\frac{\partial^2 T_0}{\partial x^2} + \frac{R_\omega}{2}\frac{\partial^2 T_0}{\partial y^2} = 0 \tag{9}$$

with boundary conditions:

$$T_0(x,0) = \tfrac{1}{2}\exp(ix)$$
$$T_0(x,y\to\infty) = 0$$
$$T_0(0,y) = T_0(2n\pi,y)$$

This expression represents the steady component of the temperature distribution and describes heat diffusion into a stagnant fluid. The order one correction to the stagnant temperature distribution is obtained by grouping the terms that contain the parameter ϵ to the first power:

$$\frac{\partial T_1}{\partial t} + u \frac{\partial T_0}{\partial x} = \frac{1}{PrR_\omega} \frac{\partial^2 T_1}{\partial x^2} + \frac{1}{2Pr} \frac{\partial^2 T_1}{\partial y^2}. \tag{10}$$

The boundary conditions are

$$T_1(x, 0, t) = 0$$
$$T_1(x, y \to \infty, t) = 0$$
$$T_1(0, y, t) = T_1(2n\pi, y, t)$$

The solution to the zero order (Eq. (9)) with corresponding boundary conditions is

$$T_0(x, y) = \tfrac{1}{2} \exp(-\alpha y \pm \mathrm{i}x) \tag{11}$$

Here $\alpha = \sqrt{2/R_\omega} = \delta/\lambda$ is the ratio of the Stokes penetration depth to the wavelength of the temperature distribution at the wall. Since the boundary condition for $y = 0$ is an even function of the axial coordinate, the solution can be formally written with a $\pm$ sign. Although it is a trivial observation at this point, it will be important in the discussion of the first-order solution.

The solution to Eq. (10) with initial and boundary conditions is composed by a transient term which is influenced by the initial conditions, and a steady-periodic term which is dominant at long enough times for the system to become periodic. The solution at long times is

$$T_1(x, y, t) = Af(y) \exp(\mathrm{i}(t + x)) + Bf(y) \exp(\mathrm{i}(t - x)) \tag{12}$$

the constants A, B are 0, ± 1, but not simultaneously zero and $f(y)$ is

$$f(y) = \frac{\exp(-\gamma y) - \exp(-\alpha y)}{2}$$
$$+ \mathrm{i}Pr \left(\frac{\exp(-\gamma y) - \exp(-(\alpha + c)y)}{2(\alpha + \mathrm{i}(1 - Pr + \alpha))} \right) \tag{13}$$

where $c = 1 + \mathrm{i}$ and $\gamma = \alpha\sqrt{1 + \mathrm{i}R_\omega Pr}$.

From Eq. (12), it is seen that there are two linearly independent solutions corresponding to left and right traveling waves respectively. The specific choice of one of them is determined by the boundary conditions at fixed x. Here we are considering cyclic boundary conditions in the axial direction and therefore traveling waves in either direction are solutions. Also the particular case of a standing wave, $A = B$ is a solution for the present boundary conditions. In the discussion of this section, we will consider in all cases $A = 1$, $B = 0$. Solutions for $A = 0$, $B = 1$, are obtained by the transformation $x \to -x$ and $T_1 \to -T_1$.

Figs. 2–5 give graphical information on the T_1 temperature field defined in Eqs. (12) and (13). In all cases, T_1 is a damped oscillatory function of the transverse coordinate.

Fig. 2 shows isotherms for $R_\omega = 50$ and $Pr = 0.1$. The positive and negative temperature zones occupy equal
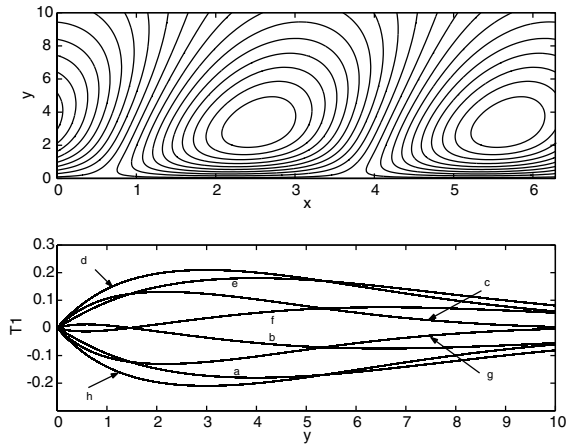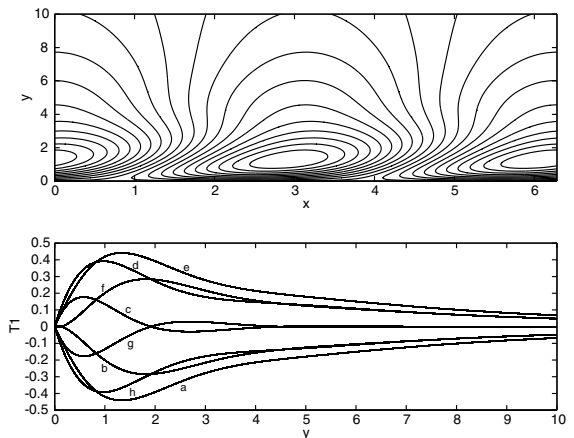

Fig. 2. Upper panel: Isotherms for $t = 0$. Lower panel: Temperature as a function of the transverse coordinate y for selected axial positions and $t = 0$. (a) $x = 0$, (b) $x = \pi/4$, (c) $x = \pi/2$, (d) $x = 3\pi/4$, (e) $x = \pi$, (f) $x = 5\pi/4$, (g) $x = 6\pi/4$, (h) $x = 7\pi/4$. $R_\omega = 50$, $Pr = 0.1$, $\epsilon \ll 1$.

Fig. 3. Upper panel: Isotherms for $t = 0$. Lower panel: Temperature as a function of the transverse coordinate y for selected axial positions and $t = 0$. (a) $x = 0$, (b) $x = \pi/4$, (c) $x = \pi/2$, (d) $x = 3\pi/4$, (e) $x = \pi$, (f) $x = 5\pi/4$, (g) $x = 6\pi/4$, (h) $x = 7\pi/4$. $R_\omega = 50$, $Pr = 1$, $\epsilon \ll 1$.

areas in the xy space, but the separatrixes between regions are inclined lines for the phase angle of the cycle considered ($t = 0$). As commented before, the symmetric temperature distribution with separatrixes inclined at opposite angles corresponding traveling waves moving to the right is obtained taking $A = 0$, $B = 1$. The distance from the wall at which T_1 reaches the first maximum is approximately $y = 3$. Given the scaling, the dynamic boundary layer or Stokes penetration depth is $y = 1$. Therefore, the thermal boundary layer extends further inward than the dynamic boundary layer, which
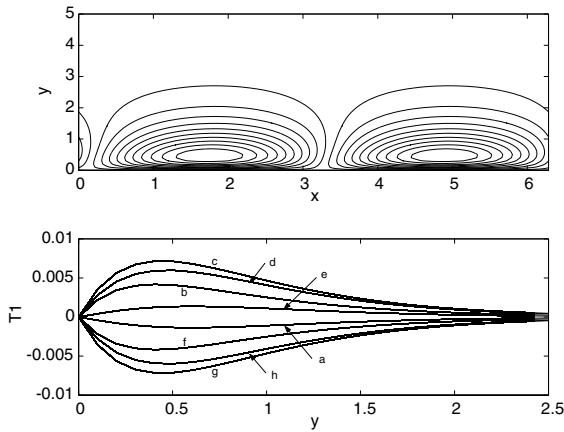
Fig. 4. Upper panel: Isotherms for $t = 0$. Lower panel: Temperature as a function of the transverse coordinate y for selected axial positions and $t = 0$. (a) $x = 0$, (b) $x = \pi/4$, (c) $x = \pi/2$, (d) $x = 3\pi/4$, (e) $x = \pi$, (f) $x = 5\pi/4$, (g) $x = 6\pi/4$, (h) $x = 7\pi/4$. $R_\omega = 5$, $Pr = 0.1$, $\epsilon \ll 1$.

is to be expected since $Pr < 1$. The corresponding information for $R_\omega = 50$ and $Pr = 1.0$ is shown in Fig. 3. The relative size of the dynamic and thermal boundary layer is about the same as in the previous case, but the

temperature fluctuations are larger. Also, in this case, the maximum temperature is found at a larger x ($x \sim \pi$). Temperature field for $R_\omega = 5$ and $Pr = 0.1$ are shown in Fig. 4. As expected, the temperature distribution is less influenced by the oscillation of the fluid. Also, note that the temperature fluctuations are about 2% of the corresponding value obtained in the case $R_\omega = 10$ and are reached nearer to the wall ($y = 0.4$).

When $A = B$ in Eq. (12), we get an standing wave as illustrated in Fig. 5 for $R_\omega = 50$, $Pr = 1$. The lines separating the hot and cold regions are vertical lines centered at the positions where the boundary condition is zero. In the interval $0 < t < 1.80$, the temporal distribution evolves in a diffusive manner, and at $t \sim 2.65$, the cold and hot regions switch places in a relative short time and then the cycle starts again.

Referring back to Eq. (8), the only term that has been neglected is $u \partial T_1/\partial x$. The magnitude of this term can be checked to estimate the error and indicate when the linearization approximation breaks down.

4. Numerical solution for arbitrary ϵ

In the previous section we studied the case when the oscillatory velocity was small ($\epsilon \ll 1$), and the resultant
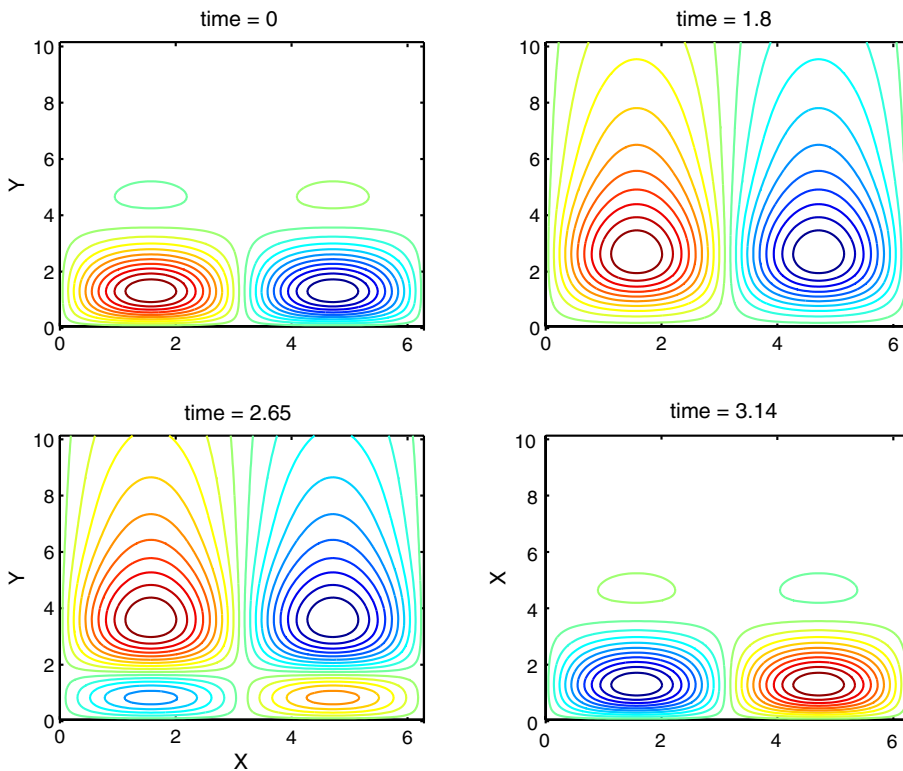

Fig. 5. Snapshots of temperature distribution, T_1, $R_\omega = 50$, $Pr = 1$, $\epsilon \ll 1$ for half a cycle of the forcing.

temperature field was only a slight departure from the diffusive solution. In this section, we relax these conditions and numerically solve Eq. (3) for unrestricted ϵ. The geometry and boundary conditions are the same as those considered in Section 1.

The numerical solution is sought by a spectral expansion of the temperature field according to

$$T(x,y,t) = \sum_{n}^{N_x} \sum_{m}^{N_y} A_{n,m}(t) R_m(y) e^{inx} \qquad (14)$$

where N_x and N_y are the number of modes in the finite expansion and $R_m(y)$ are rational Chebyshev polynomials [13]. Rational Chebyshev polynomials are useful for employing spectral methods in semi-infinite domains. The polynomials are simply a transformation of standard Chebyshev polynomials and the algorithms for using these polynomials are identical to spectral methods based on Chebyshev polynomials. Rational Chebyshev polynomials are related to regular Chebyshev polynomials by the relation,

$$R_m(y) = T_n(\hat{y}) \qquad (15)$$

where

$$y = L(1+\hat{y})/(1-\hat{y}), \qquad (16)$$

and L is the boundary layer thickness map parameter; we use $L = 5$ in our simulations but the results are not sensitive to the value. The rational Chebyshev transformation simply stretches the grid points from the usual $-1 < y < 1$ domain to $0 < y < \infty$ while clustering most of the grid points between $0 < y < L$.

After applying the expansion, the governing equation becomes a set of ordinary differential equations for the expansion coefficients, $A_{m,n}$. The equations are integrated forward in time using a fractional step method. The convective term is integrated using an Adams–Bashforth method while the diffusive term is integrated with a simple implicit backward-Euler approximation to ensure numerical stability. The convective term was computed using the usual pseudo-spectral approximation: derivatives are computed in function space, the results are transformed to physical space, the product is taken in physical space, and the final result is transformed back to function space [14].

The boundary conditions are imposed by enforcing the temperature at the plate and at the last grid point in the y direction, which is typically $y = 10^4$ (but depends on how many points are used in the expansion). The choice of expanding the x direction with a Fourier series automatically satisfies the periodicity boundary condition in this direction. The initial condition for the simulation was the total temperature set to zero everywhere in the domain. The numerical method was validated by employing standard convergence tests as well as comparing the exact analytical diffusive solutions to the

simulations. The method was found to be both efficient and accurate, complete results can be obtained in only a few seconds on a standard PC, $N_x = N_y = 32$ provided an adequate resolution.

4.1. Transient behavior

We compared the numerical to the analytical solutions for small ϵ to validate the methods and analyze the transient behavior. The temperature field goes through a brief transient then reaches a steady state with periodic dynamics. When viewing the solution as the departure from the diffusive solution we find that the standing wave solution (i.e. $A = B$) is the long term solution. Using an $\epsilon = 0.1$ we found that the numerical and analytical expressions matched well within 1% after the transient has decayed.

Typical transient behavior is shown in the following sequence of figures. In Fig. 6 we show the temperature contours in the x–y plane at four instances in time for the case of $Re = 50$, $Pr = 1$, $\epsilon = 0.1$. These snapshots are taken when the flow is still undergoing the transient. Corresponding to these snapshots is Fig. 7, where we show the temperature at a single location as a function of time. In this figure we clearly see the transient and transition to periodic dynamics. The "stars" in Fig. 7 represent the times for the four snapshot frames in Fig. 6.

An alternate view of the transient phenomena is shown in Fig. 8. In this figure we plot the image of T_1 along a single vertical location ($y = 2$) at each instant in time. This plot has the same parameters as Figs. 7 and 6. In this figure we can clearly see the development of the periodic standing wave at late times. The standing wave is found to center at the locations where temperature boundary condition, $\cos(x)$, is equal to zero. The period of the oscillation is driven by the oscillatory flow and taking a power spectrum in time shows that the only significant frequency component of the flow is at $\omega = 2\pi$. The final flow that develops is found to perfectly agree with the analytical standing wave solution provided in the previous section.

4.2. Solution at long times

The general development of the temperature field is similar as the flow velocity is increased. The temperature goes through a transient and evolves to a state of periodic dynamics. As the magnitude of the oscillatory flow is increased, the dynamics become more complex and more frequency and wavenumber components become involved in the final solution. In Fig. 9 we show the data in the same method as in Fig. 8, only we have increased the flow velocity to $\epsilon = 1.0$. In this case we see that the temperature dynamics become somewhat more complex,
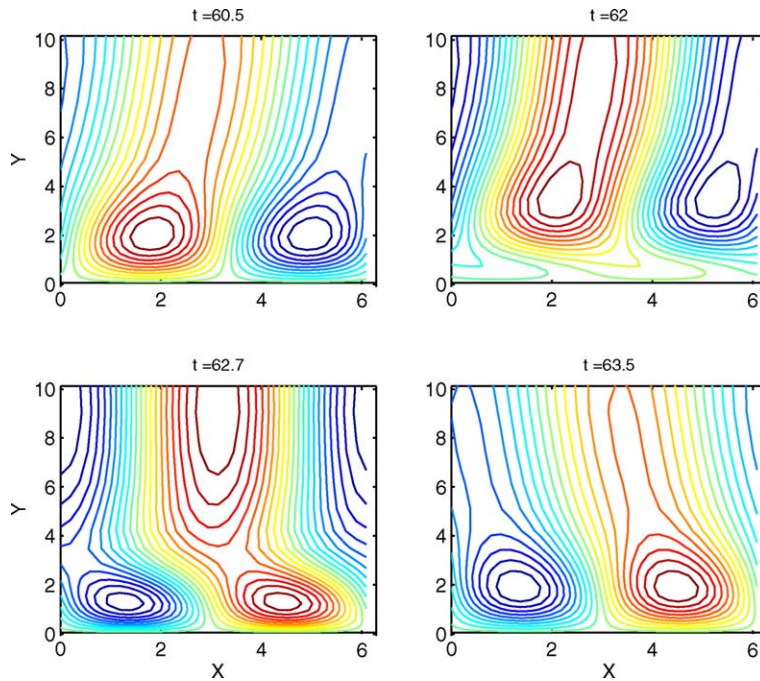
Fig. 6. The temperature field contours (the diffusive solution has been subtracted) at four instances in time. The four snapshots correspond to the '*' points in Fig. 7. The solution is still in the transient stage and is on the way evolving to a pure standing wave.
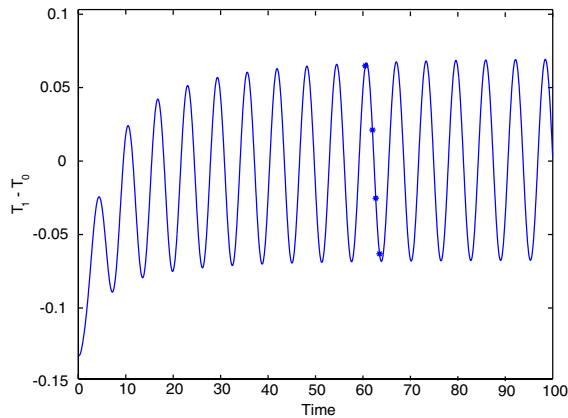

Fig. 7. The temperature at a single point, $x = \pi/2$ and $y = 2$, as a function of time. The figure shows a transient followed at long times by periodic dynamics.
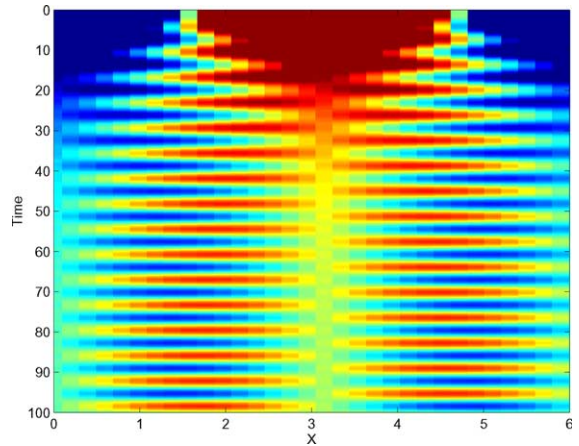

Fig. 8. Temperature, T_1, at $y = 2$ as a function of time for $\epsilon = 0.1$. The magnitude of the temperature is imaged such that red is greater than the diffusive solution (hot) and blue is less than the diffusive solution (cold). The image shows the transient development and the evolution to the standing wave solution centered at the zeros of the boundary condition. (For interpretation of the references in color in this figure legend, the reader is referred to the web version of this article.)

though there is still only the presence of the standing wave with the temporal frequency of the flow oscillation.

As the flow velocity is further increased more temporal and spatial frequencies become present in the solution. Another method to visualize the temporal dynamics is to plot the temperature at two different physical locations in the domain at each instant in time. We select points at $x = \pi/2$ and $y = 0.15$, $y = 2.0$ and

plot the values of T_1 at each instant in time. The result for different flow velocities is shown in Fig. 10. We see more and more complex dynamics as the flow rate is increased. At the lowest flow rates we see that only one
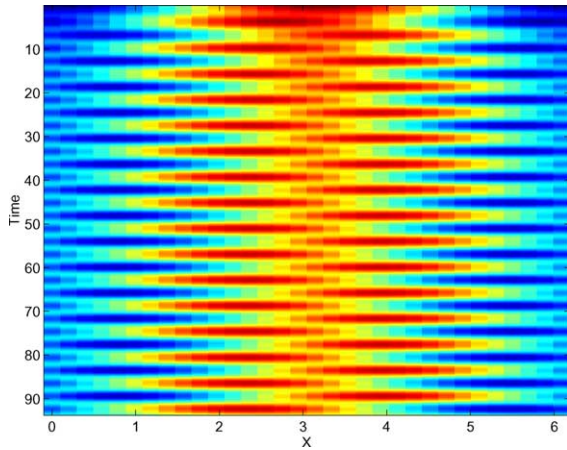
Fig. 9. Temperature, T_1, at $y = 2$ as a function of time for $\epsilon = 1.0$. The magnitude of the temperature is imaged such that red is greater than the diffusive solution (hot) and blue is less than the diffusive solution (cold). The image shows the rapid transient development and the evolution to the standing wave solution. (For interpretation of the references in color in this figure legend, the reader is referred to the web version of this article.)
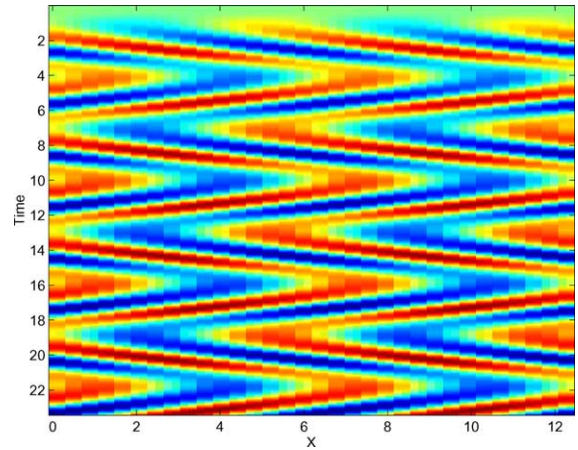

Fig. 10. Temperature at two locations, $(x = \pi/2, y = 0.15)$ and $(x = \pi/2, y = 2)$, at each instant in time. The flow velocity is increased throughout the four plots. At the lowest velocities, $\epsilon = 1$, we see only one frequency is dominant since the values trace out an ellipse. As the velocity increases there are clearly more frequencies present in the dynamics.

temporal frequency is present, just as with the $\epsilon \ll 1$ analytical solution the plot traces an ellipse. At the highest flow rate shown the dynamics become quite complex and more temporal frequencies are evident.

While the dynamics at the highest velocities have many spatial and temporal frequencies present the solutions seem quite logical when we view the develop-

Fig. 11. Total temperature, $T_0 + T_1$, at $y = 2$ as a function of time for $\epsilon = 4.0$ The image shows the rapid transient development and the evolution to the oscillation from the flow forcing.
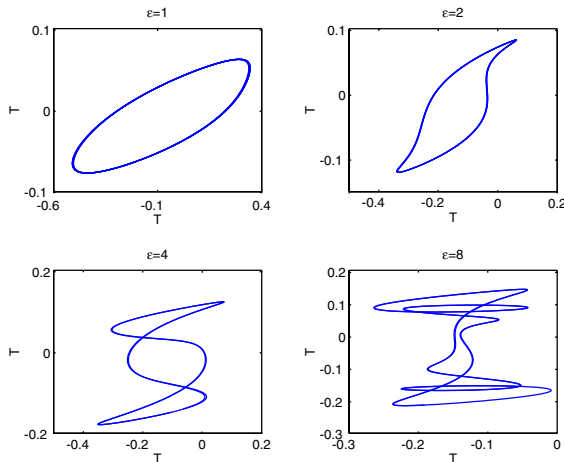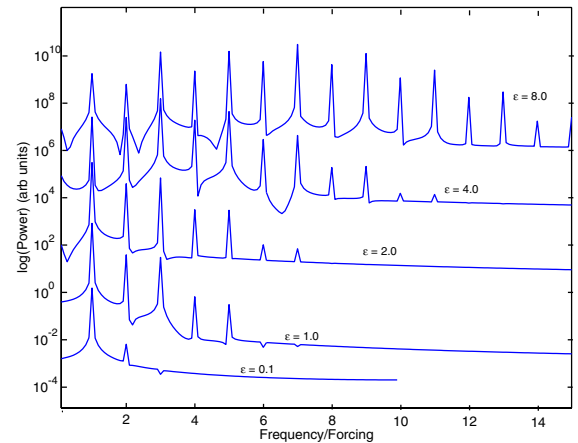

Fig. 12. Fourier power spectrum of the temperature history at $x = \pi/2$, $y = 2$ for different values of $\epsilon = 0.1$, 1, 2, 4 and 8. The power is arbitrary and each curve is shifted upward in order to visualize the features are different ϵ. A salient feature of the plot is that only harmonics of the forcing are present.

ment of the complete temperature field $(T_0 + T_1)$ rather than as the departure from the diffusive solution. Using the same method of visualization as in Figs. 8 and 9, we plot the total temperature field for $\epsilon = 4$ in Fig. 11. In this figure we clearly see convection of the temperature field as a forced flow oscillates. The increase in the number of frequencies present in the solution is further illustrated in Fig. 12 where the time-Fourier spectrum of the temperature is shown for $x = \pi/2$, $y = 2$ and $\epsilon = 0.1$, 1, 2, 4 and 8. A salient feature of the plot is that only harmonics of the forcing are present. As commented before, for the smallest ϵ, the only relevant frequency corresponds to the forcing. As ϵ is increased, more

harmonics become important and for $\epsilon = 4$, the dominant frequency is not the forcing but its third harmonic. Further increase in ϵ results in several dominant harmonics.

5. Heat transfer

The instantaneous and local heat transfer is $q = -k \frac{\partial T}{\partial y}\big|_{y=0}$ and can be easily calculated from the analysis presented above. We present the heat transfer results using the standard definition of the Nusselt number; $Nu = q\delta/kT_{\mathrm{w}}$. In the present context the useful definition is the Nusselt number averaged over half the axial wave length and one temporal cycle i.e.

$$\langle \overline{Nu} \rangle = \int_0^\pi \left[\int_{-\pi/2}^{\pi/2} \left(-\frac{\delta}{kT_{\mathrm{w}}} \frac{\partial T_1}{\partial y}\bigg|_{y=0} \right) \mathrm{d}x \right] \mathrm{d}t \qquad (17)$$

For the $\epsilon \ll 1$ case, it is easy to see that since $T_1 = f(y) \exp(\mathrm{i}(x+t))$, then $\langle \overline{Nu} \rangle = 0$. The modification of the heat transferred to or from the wall brought by the correction T_1 in the first half a cycle is compensated by an identical amount with the opposite sign in the second half of the cycle. In the general case, for arbitrary values of ϵ, the heat transfer is also zero. This is to be expected since the boundary condition is periodic in x and the forcing is periodic in time and independent of x.

The time-dependent, space-averaged Nusselt number defined as the expression in the square brackets in Eq. (17), displays an interesting behavior. Upon using Eqs. (12) and (13) with $A = 1$, $B = 0$, we get

$$\langle Nu \rangle = \int_{-\pi/2}^{\pi/2} \left(-\frac{\delta}{kT_{\mathrm{w}}} \frac{\partial T_1}{\partial y}\bigg|_{y=0} \right) \mathrm{d}x$$
$$= -\frac{2\delta}{kT_{\mathrm{w}}} (-I_1 \cos t + I_2 \sin t), \qquad (18)$$

where

$$I_1 = \frac{\alpha - \gamma_R}{2} + \frac{Pr}{2} \left(\frac{-\alpha + \gamma_I \alpha + (\alpha + 1 - \gamma_R)(1 - Pr + \alpha)}{\alpha^2 + (1 - Pr + \alpha)^2} \right)$$

and

$$I_2 = \frac{\gamma_I}{2} - \frac{Pr}{2} \left(\frac{(\alpha + 1 - \gamma_R)\alpha + (1 - \gamma_I)(1 - Pr + \alpha)}{\alpha^2 + (1 - Pr + \alpha)^2} \right).$$

Here, the real and imaginary parts of γ are

$$\gamma_R + \mathrm{i}\gamma_I = \alpha \sqrt[4]{1 + R_\omega^2 Pr^2}(\cos\theta + \mathrm{i}\sin\theta).$$

and $\theta = R_\omega Pr$.

Eq. (18) indicates that the relative phase between $\langle Nu \rangle$ and the velocity oscillation depends on R_ω and Pr.

For instance, when Pr is very large and R_ω is moderate, $I_1 = I_2 = -\sqrt{Pr}/2$ and the relative phase is $\pi/4$. In contrast, for $Pr \to 0$, as is approximately the case for liquid metals, $\langle Nu \rangle$ vanishes.

6. Concluding remarks

The problem of two competing–complementing heat transfer mechanisms of conduction in the transverse direction and forced convection in the axial direction has been analyzed. The specific problem analyzed is the heat transfer of an oscillatory flow in contact with a wall with a sinusoidal temperature distribution. Considering only the case where the ratio of the axial velocity to the product of the oscillation frequency times the wave length of the wall temperature distribution is small, an analytical solution has been obtained. It was found that for $Pr = 1$, the convective effect has maximum influence at a distance of one Stokes penetration depth. The equivalent problem with arbitrary free stream velocity was solved with a numerical method. The numerical integration revealed that the temperature distribution in the transient state is similar to a traveling wave, while the long term solution is a standing wave. The heat transfer from the boundary to the fluid is always zero. The results of this paper have assumed that the base flow is stable [15], that natural convection effects are negligible, and that the flow is two-dimensional. These assumptions should always be checked before applying the analysis presented here. Natural convection in two dimensions has been incorporated into many heat transfer studies (see for instance [16]) and its inclusion in the oscillatory boundary layer flow is a topic of future work. Furthermore, three-dimensional effects can have a large influence on heat transfer rates [17] but a corresponding analysis incorporating oscillatory flows would require more sophisticated numerical and analytical models than those presented here.

References

[1] W.L. Cooper, V.W. Nee, K.T. Yang, Fluid mechanics of oscillatory and modulated flows and associated applications in heat and mass transfer—a review, J. Energy, Heat and Mass Transfer 15 (1993) 1–19.

[2] T.S. Zhao, P. Cheng, Heat transfer in oscillatory flows, in: C.-L. Tien (Ed.), Annual Review of Heat Transfer, vol. IX, 1998 (Chapter 7).

[3] S. Goldstein (Ed.), Modern Developments in Fluid Mechanics, vol. II, Dover, New York, 1965.

[4] T.S. Zhao, P. Cheng, A numerical solution for laminar forced convection in a heated tube subjected to a periodically reversing flow, Int. J. Heat Mass Transfer 38 (16) (1995) 3011–3022.

[5] T.S. Zhao, P. Cheng, Oscillatory heat transfer in a pipe subjected to a laminar reciprocating flow, J. Heat Transfer 118 (1996) 592–597.

[6] U.H. Kurzweg, Enhanced heat conduction in oscillating viscous flows within parallel-plate channels, J. Fluid Mech. 156 (2) (1985) 291–300.

[7] U.H. Kurzweg, Temporal and spatial distribution of heat flux in oscillating flow subjected to an axial temperature gradient, Int. J. Heat Mass Transfer 29 (12) (1986) 1969–1977.

[8] U.H. Kurzweg, J. Chen, Heat transfer along an oscillating flat plate, J. Heat Transfer 110 (8) (1988) 789–790.

[9] P. Li, K.T. Yang, Mechanisms for the heat transfer enhancements in zero-mean oscillatory flows in short channels, Int. J. Heat Mass Transfer 43 (2000) 3551–3566.

[10] D.-Y. Lee, S.-J. Park, S.T. Ro, Heat transfer by oscillating flow in a circular pipe with a sinusoidal wall temperature distribution, Int. J. Heat Mass Transfer 38 (14) (1995) 2529–2537.

[11] A. Mandelis, Diffusion-Wave Fields, Springer, 2001.

[12] I.G. Currie, Fundamental mechanics of fluids, McGraw-Hill, 1993.

[13] J.P. Boyd, Orthogonal rational functions on a semi-infinite interval, J. Comput. Phys. 70 (1987) 62–88.

[14] B. Fornberg, Practical Guide to Pseudospectral Methods, Cambridge University Press, 1996.

[15] S.H. Davis, The stability of time-periodic flows, Ann. Rev. Fluid Mech. 8 (1976) 57–74.

[16] K. Khanafer, K. Vafai, M. Lightstone, Mixed convection heat transfer in two dimensional open ended enclosures, Int. J. Heat Mass Transfer 45 (2002) 5171–5190.

[17] M.P. Dyko, K. Vafai, Three-dimensional natural convective states in a narrow gap horizontal annulus, J. Fluid Mech. 445 (2001) 1–36.